Conf-740316--3

PROPERTIES OF RF-CONFINED PLASMAS

by

Albert J. Hatch

Presented at:

Conference on Electrostatic and Electromagnetic Confinement of Plasmas and the Phenomenology of Relativistic Electron Beams, New York, New York, March 4-7, 1974

U of C-AUA-USAEC

ARGONNE NATIONAL LABORATORY, ARGONNE, ILLINOIS

PROPERTIES OF RF - CONFINED PLASMAS*†

Albert J. Hatch

Physics Division, Argonne National Laboratory, Argonne,

Illinois 60439

Abstract

An experimental study has been made which confirms the theoretical prediction of confinement of low-density plasmas ($n<n_c$) at sufficiently low pressure in an electric quadrupole field having a Φ potential well. A cylindrical resonant cavity 36 cm in diameter and 24 cm long was used. When excited in the electric dipole TM_{010} mode (nonconfining) at 644 MHz, no breakdown or discharge could be observed at pressures below that corresponding to the electron mean-free-path limit of the diffusion mechanism of rf breakdown. However, when excited in the electric quadrupole TM_{011} mode (confining) at 902 MHz, breakdown and discharge were observed at pressures down to 3 decades below the m. -f. -p. limit. Observations of the discharge luminosity in the TM_{011} mode showed a minimum at the center of the Φ well at a pressure above the m. -f. -p. limit and a maximum below the limit. As pressure was reduced, the floating potential of a probe at the center of the Φ well showed a change from + to - at a pressure about 1 decade below the m. -f. -p. limit. A simple analysis of stochastic heating of electrons by collisions with neutrals indicates that the cycling "lifetime" of confined electrons is of the order of microseconds.

*Work performed under the auspices of the U.S. Atomic Energy Commission.

†Paper 24, Conference on Electrostatic and Electromagnetic Confinement of Plasmas and the Phenomenology of Relativistic Electron Beams, sponsored by the New York Academy of Sciences, New York, N.Y., March 4-7, 1974.

1. Introduction

The research that I will describe was begun in ~1960 with an analytic study, was continued intermittently through the 1960's with the assembly and commissioning of an experimental facility, and came to partial fruition in 1971-72 with results that have been partially published. This rf-confinement research was a relatively small part of a broader study of plasmas produced in rf and microwave cavity fields. The present paper contains a summary of some of these earlier studies and results, plus additional new results.

Prior to our experimental work described here, the only experimental study of rf confinement per se was by Self and Boot[1] in 1959. However, their investigations were limited to breakdown and did not include any observations or measurements of plasma properties. Our breakdown results, reported earlier[2,3] and summarized here, are an extension of the work of Self and Boot. Our new results described here include measurements of the luminosity distribution (reported in part earlier[2,3]), and the floating potential of the confined plasma.

2. Theoretical Considerations

From the early theoretical studies of rf confinement of plasmas[4-6], it became clear that the Φ-quasipotential method[7] was at once both simple and useful. Thus, the total energy of an electron could be represented by the period-averaged oscillatory energy $\Phi = e^2E^2/4m\omega^2$ resulting from its direct interaction with the rf field,

plus any slowly-varying drift kinetic energy T resulting from either an initial drift motion, from drift motion arising from the drift force $\mathfrak{F} = -\nabla\Phi$, or from a combination of both. For the collisionless case the system is conservative, and hence $\Phi + T = \text{constant}$. The condition for confinement is that the electron be in a Φ well having a rim of effective depth $\Phi_R > \Phi + T$. From the topology of Φ in rf fields it is easily shown that there is no Φ well in a field of the electric dipole generic type, but that a Φ well does occur in the vicinity of the central nodal-point of an electric quadrupole field. If the field is to act on the electron, then the density must be below cutoff, i.e. $n < n_c = \omega^2 m\epsilon_o/e^2$, where $\omega = 2\pi f$ is the radian frequency of the field, m and e are the mass and charge of the electron, respectively, and ϵ_o is the permittivity of free space.

The correspondence between the topology of the Φ well and the field configuration in the TM_{011} electric quadrupole mode of a cylindrical cavity is shown in Fig. 1.[8,9] These plots are for a cavity having a diameter/length ratio D/L = 3/2, a value chosen for our work on the basis that it gives the maximum well depth per unit of rf power. The effective depth of the Φ well corresponds to the value Φ_R at the rim isopotential which passes through the saddle point S shown in Fig. 1(a). The 3-dimensional shape of the well is approximately that of a cylinder coaxial with the cavity as indicated in Fig. 1(b). The volume of this Φ well is approximately 12% that of the cavity.

Figure 2 is a plot of a computer-simulated trajectory of a single electron confined in the axial midplane of the TM_{011} mode of the 36 × 24 cm cylindrical cavity used in this work. This plot was generated in a manner similar to that described in the earlier paper by Dr. Shohet[10], except that the cylindrical cavity fields were used here. The electron was launched with 0 drift speed (quiet start) at the point indicated by the arrows at the lower right.

3. Experimental System

The rationale involved in the basic design of our experimental facility can be summarized as follows:

First, a cylindrical shape cavity was selected because of its (a) circular symmetry, (b) fixed axis of symmetry, and (c) ease of fabrication. A rectangular cavity fails to meet requirements (a) and (c); a spherical cavity fails to meet requirements (b) and (c).

Second, the relative dimensions of the cylindrical cavity were determined by consideration of the dependence of the depth of the Φ well on the D/L ratio. A computational study of the depth of the Φ well as a function of D/L gave the results that the maximum depth occurs at D/L = 3/2, and hence this ratio was used.

Third, the commercial UHF-TV band (~400-1000 MHz) was chosen as the approximate frequency range to be used mainly because a large cavity would facilitate optical observation and other

studies of the properties of the large-volume confined plasma. (Self and Boot used a cavity excited at 8.7 GHz in which the volume of the Φ potential well was only ~ 3 cm^3; the corresponding volume in our cavity is ~ 3 liters.) An additional practical consideration was the ready commercial availability of medium-power microwave equipment in the UHF-TV band.

Fourth, the absolute size of the cavity was determined so that we could use a single UHF power source that was tunable through a frequency range wide enough to excite either of the TM_{010} or TM_{011} modes separately in a single cavity. A compatible system was found to be one using an Eimac 4KM3000LR klystron tube, which has a nominal frequency range of 610—985 MHz and a cw power rating of 2000 W, in conjunction with a cylindrical cavity having D = 36 cm and L = 24 cm for which the frequencies of the TM_{010} and TM_{011} modes were calculated to be 638 and 893 MHz, respectively. For a copper cavity of these dimensions, the theoretical Q of the TM_{011} mode is 33 000 and the depth of the Φ well is 164 eV at rated klystron power.

Figure 3 shows an axial midplane cross section of the cavity used and Fig. 4 is a photograph of the cavity. All interior surfaces were OFHC copper clad to an exterior vacuum shell of stainless steel except the bottom copper end plate which was perforated with 1/8-in. diameter holes to act as pumping ducts having a minimum perturbing effect on the cavity field. The cavity was watercooled and Viton 'O' rings were used throughout except at the Pyrex viewing

window where a copper gasket was used. The cavity "field meter" was based on the sensing magnetic loop in the upper right corner of the cavity having its plane in an axial plane of the cavity and being connected to the RF VTVM. Calibration of this field meter was accomplished by use of the TM_{010} mode and an upper end plate which had a small capacitor-dividing voltmeter that had been calibrated independently by a capacitance meter at a low non-resonant frequency. This calibration was verified independently by use of the TM_{010} mode and the relation $E_o = (2\ PQ/\omega\ \eta)^{1/2}$ where P is the input power in watts, and η is a readily-calculated geometrical factor.[11] Experimental error in the measurement of E_o was attributed to error in measurement of the capacitance ratio in the first case and to error in measurement of Q in the second case. The resultant absolute error in E_o was estimated to be ± 10%, giving an error in the depth Φ_R of the confining potential well of ±20%. However, the relative error in E field values was smaller, ~±3%.

A block diagram of the experimental system is shown in Fig. 5. The klystron power amplifier using the 4KM3000LR 4-cavity aircooled klystron tube was built to our specifications by Continental Electronics, a firm specializing in high-power radar systems and rf particle accelerators. Driving power was furnished by a Sierra Model 470A-1000 power oscillator. Output power could be varied smoothly and continuously from 0 to 2000 W by varying klystron beam voltage.

Frequency could be shifted while maintaining nearly constant output power by use of remotely-driven klystron tuning cavities. Impedance matching was greatly facilitated by use of an Alford automatic impedance plotter. A photograph of the experimental system is shown in Fig. 6.

4. Experimental Results

a. Breakdown

Breakdown curves for both the TM_{010} and the TM_{011} modes are shown in Fig. 7. These measurements were made by Rev. Charles Shelby and used in his thesis.[2] The TM_{011} curve has been published.[3] The abrupt cutoff in the breakdown curve for the TM_{010} mode near the predicted electron mean-free-path limit of the diffusion mechanism[12] was readily reproducible and very sharp. Its onset could be precipitated by reducing pressure from 3.0 mT to 2.8 mT, whereupon the cavity field could be increased by a factor of ≥ 10 without breakdown occurring, the field being limited only by breakdown at atmospheric pressure in the exterior tuning stubs. The electron mean-free-path limit is defined as the condition for which the m.-f.-p. λ_e equals the characteristic diffusion length Λ of the cavity. For this cavity, $\Lambda = 5.29$ cm. For air, $\lambda_e = 0.026/p$.

No such cutoff was ever observed for the TM_{011} mode. Instead, the breakdown curve continued its logarithmically linear rise with decreasing pressure for nearly a decade below the m.-f.-p. limit, whereupon it underwent a smooth transition to a slightly rising plateau at a field strength level corresponding to a Φ-well depth of $\sim$15—35 eV.

This plateau region is the regime of rf-confinement-aided breakdown. Here the electrons (on the average) do not escape from the interior field regions of the cavity before undergoing an ionizing collision as happens in the TM_{010} mode, but instead are kept in the Φ well region long enough for such collisions to occur. In this extension of the work of Self and Boot we have definitely established the existence of the plateau characteristics of rf-confinement-aided breakdown and have shown that the level of this plateau corresponds to Φ well depths of $\geq 1—2\ 1/2$ times the ionization potential of the gas.

b. Luminosity Measurements

In the electron diffusion mechanism of rf breakdown the ionization coefficient depends on a positive power of the electric field[13], and hence it is not at all surprising that in weakly-ionized gas discharges the luminosity is also dependent on both the field and on the existing electron density. A brief digression will serve to illustrate this point.

Clear evidence of the correlation between luminosity and field is given by the photographs and related field patterns shown in Fig. 8 for three modes of a resonant cavity ircluding those described above. This particular cavity (built for other purposes) had a cylindrical wall made of perforated copper so that it was semi-transparent to visible light but nearly opaque to microwaves. The cavity was 33 cm in diameter and 42 cm long and was excited by the same microwave power system shown in Fig. 5. Low pressure for the discharge was maintained by use of a Pyrex liner inside the perforated copper. All the

photographs were taken at pressures in the vicinity of the collision-frequency transition pressure ($\sim$ 1 Torr) for each mode, approximately at the minimum in the breakdown curve. In each case of these diffusion-cominated discharges the region of maximum luminosity corresponds to the region of maximum electric field. The reader's attention is called to the photograph and field illustrations for the TM_{011} mode - the confining mode. In this case where the field strength corresponds to the minimum in the breakdown curve at which the Φ well depth is ≤ 0.1 eV, no confinement effects were observed. That is, there was no discernable glow at the central nodal point of the cavity which is also the center of the Φ well. The glow was highly localized at the two ends of the cavity. As pressure was reduced one or two decades, the glow gradually filled the rest of the tube but the maximum luminosity stayed at the two ends. The pressure in this system was never reduced to that corresponding to the rf confinement domain. The point of this digression, then, is that in the diffusion mechanism there is a strong correlation between electric field, luminosity, and electron (plasma) density.

Now we return to the main theme of this paper. Luminosity measurements were made using the pivoted photometer arrangement shown in Fig. 9. The photometer had a narrow field of view ($\sim 1\text{-}2^{\circ}$ angle of acceptance) and was pivoted about a horizontal axis that passed through an opening in the perforated copper wall section of the cavity. Thus, as the photometer was scanned slowly between the limiting small

values of vertical angle θ, the resulting trace on the X-Y plotter could be considered as an axial profile of luminosity.

Two profiles obtained in this way are shown in Fig. 10. Both are for the quadrupole TM_{011} mode. Trace A was obtained at conditions corresponding to A in Fig. 7, and hence represents a diffusion-controlled plasma. The minimum in this trace near the central nodal point of the mode is consistent with the luminosity distribution for the TM_{011} mode in Fig. 8. Trace B, however, was obtained at conditions corresponding to B on the plateau in Fig. 7, and hence can be considered as representing an rf-confined plasma. The maximum luminosity near the central nodal point is contra-indicative of a typical diffusion-controlled plasma. It is interpreted as indicating the presence of an rf-confined plasma located mainly in the Φ well and having its maximum density at the nodal point center of the Φ well. About 1 minute was required to obtain each luminosity profile of these steady-state plasmas.

c. Plasma Floating Potential

Since $\Phi = e^2E^2/4\,m\omega^2$ varies inversely as mass, then it appears that the confining effect of a Φ-potential field should be exerted primarily on the electrons and that the ions should be held in the well secondarily by time-average space-charge attraction to the confined electron cloud. Thus, in the rf-confinement regime both the plasma potential and the floating potential should be negative rather than positive as usually occurs in the diffusion regime. (The floating

potential is that acquired by a probe tip immersed in the plasma and measured with respect to the grounded reference of the plasma container, i.e. the cavity in this case.) To explore this hypothesis experimentally, we inserted a Pyrex-enveloped Langmuir-type tungsten probe in the cavity as shown in Fig. 11. The purpose of having the probe traverse the diagonal from a corner of the cavity to the center was to avoid the possible short-circuiting effect of a probe mounted along either the axis or a midplane diameter. The floating potential of the probe was measured with a Keithley electrometer. Measurements were made by increasing pressure while holding input rf power approximately constant at ~300 W. Typical results are shown in Fig. 12.

At the higher pressures where the diffusion mechanism is dominant the probe potential V_F is positive as one normally observes in these plasmas. This is caused by the more rapid initial transient diffusion of high-mobility electrons from the discharge region until a steady-state space-charge-dominated diffusion of both electrons and ions is established. The rise in V_F as pressure is decreased is also typical of diffusion-controlled rf discharges, especially in the low-pressure regime near the electron mean-free-path limit.

The unique result here is the rather precipitous reversal of V_F from positive to negative at a pressure ~1 1/2 decades below the m.-f.-p. limit. Note that this is also slightly below the pressure where the rf-confinement-aided plateau becomes established on the breakdown curve in Fig. 7. Below this reversal of V_F in Fig. 12 it appears that a

negative plateau is about to be established, but experimental difficulties prevented us from exploring this regime.

The main experimental difficulty encountered was that the Pyrex housing of the probe became heated in the rf field which is large near the midpoint of the diagonal section of the probe. This sometimes caused the probe to sag and it became useless. We could usually circumvent this difficulty by keeping rf power low until the pressure adjustment had been made, then increasing the power quickly and reducing it quickly after obtaining a steady-state reading. However, this modus operandi was self-limiting at the lower pressures because of the increased field required on the slowly-rising breakdown plateau. It also contributed to the rather large error indicated. The ideal solution to this problem would have been to use a quartz-enveloped probe, but this we were unable to do.

Also shown in Fig. 12 is the magnitude (in arbitrary units) of the rf field in the cavity. This was measured by the magnetic sensing field probe shown in Fig. 3. The small increase as pressure was increased initially indicates a slight retuning and/or change in impedance matching due to the presence of the plasma having an increasing but small density. As pressure is increased further the very large decrease in field (by more than a factor of 10) is due to the loading effect of the higher density plasma on the cavity. Since the plasma density in this higher pressure range is undoubtedly comparable to cutoff density, the

magnitude of field indicated at the probe position does not necessarily correspond to that in the plasma

d. Other Properties

No measurements of plasma temperature or density in the confinement regime have been made. However, from considerations of the existence of excitation and ionization energy levels in air up to about 15 eV, and of the ~15—35 eV depth of the Φ well, one would expect that the electron kinetic temperature would be in the vicinity of ~10—15 eV. Ion temperatures are undoubtedly only a small fraction of an eV. Indirect qualitative comparisons of luminosity between the present confined plasma and other rf plasmas for which the density is known (e.g., rf plasmoids), indicate that the density here is only of the order of 10^8 cm^{-3}, compared with a cutoff density of ~10^{10} cm^{-3} at 902 MHz. The Debye length corresponding to 10 eV and 10^8 cm^{-3} would be ~0.25 cm.

5. Stochastic Heating

An electron oscillating in an rf field but not undergoing collision can gain no energy from the field. However, if elastic collisions occur which are random in time phase, then the average energy gain per collision is twice the period-averaged oscillatory energy possessed by the electron before the collision.[14] Thus electron stochastic heating occurs at the rate $P_s = \nu(e^2E^2/2m\omega^2)$, where ν is the collision frequency. For an electron placed in the Φ well with an initial energy

of 1 eV (e.g., from an inelastic ionizing collision), the average energy after successive elastic collisions will be 3, 9, 27, etc. eV. Therefore, only ~3-4 collisions are required for an electron to gain enough energy to escape from the Φ well or to cause an ionizing or other inelastic collision. For air in which $\nu \approx 5 \times 10^9 p$, where p is the gas pressure in Torr, the time required for an electron to reach ionizing energy at a pressure of 0.4 m Torr (corresponding to trace B in Fig. 8) is only ~2μ sec. This is the cycling "lifetime" of an electron in the Φ well.

In order that electrons which gain more than ionizing energy not be lost from the Φ well, the well depth Φ_R must be somewhat deeper than V_i. In the present case, the maintainance of a steady-state electron population appears to require a Φ well depth of ~1—2 1/2 times the ionization potential.

6. Summary

The rf breakdown measurements of Self and Boot have been extended to lower pressures and correlated with Φ-well theory in such a way as to confirm the existence of a dominant rf-aided breakdown regime at pressures less than ~1/10 that corresponding to the electron mean-free-path limit of the electron-diffusion breakdown regime. Additional measurements of luminosity distribution and of floating potential at the center of the Φ well are consistent with the existence of quasi-steady-state rf-confined plasma. Considerations of stochastic heating lead to the conclusion that rf confinement involves a continuous

electron cycling process in which electrons gain energy through random elastic collisions and lose energy through inelastic collisions.

ACKNOWLEDGEMENTS

It is a pleasure to acknowledge the collabc ration of Rev. Chas. Shelby and his permission to use material from his M.S. Thesis. Valuable technical assistance was also provided by A. E. Froehlich.

References

1. Self, S.A. and H.A.H. Boot. 1959. J. Electron. Contr. 6: 527 - 547.

2. Shelby, C.F. 1972. Plasma Confinement in a Microwave Cavity. M.S. Thesis, De Paul University, Chicago, Ill. [Available as Argonne Physics Division Informal Report No. PHY-1971 D. December, 1971.]

3. Shelby, C. F. and A. J. Hatch. 1972. Phys. Rev. Letters. 29: 834 - 837.

4. Boot, H.A.H., S. A. Self, and R. B. R. -Shersby-Harvie. 1958. J. Electron. Contr. 4: 434 - 453.

5. Gapanov, A.V. and M.A. Miller. 1958. Zh. Eksp. Teor. Fiz. 34: 242 - [Sov. Phys. JETP 7: 168 -

6. Weibel, E.S. 1958. Confinement of a Plasma Column by Radiation Pressure. In The Plasma in a Magnetic Field. R K.M. Landshoff, Ed. 60 - 76. Stanford Univ. Press. Stanford, Calif.

7. Motz, H. and C.J.H. Watson. 1967.

In Advances in Electronics and Electron Physics. L. Marton, Ed. Vol. 23: 153 - 302. Academic Press. New York, N.Y.

8. Hatch, A.J. and M. Hasan. 1966. Proc. Nat. Electron. Conf. 22: 962 - 966.

9. Hatch, A.J., M. Hasan and W.E. Smith. 1968. Deuxième Colloque sur les Interactions entre les Champs Oscillants et les Plasmas.

3: 949 - 986. L'Institut National des Sciences et Techniques Nucléaires, Saclay.

10. Hatch, A.J. and J. L. Shohet. Phys. Fluids. To be published.

11. Rose, D.J., D. E. Kerr, M.A. Biondi, E. Everhart and S.C. Brown. 1949. Methods of Measuring the Properties of Ionized Gases at Microwave Frequencies. Tech. Rep. No. 140. Massachusetts Institute of Technology.

12. Brown, S.C. 1966. Introduction to Electrical Discharges in Gases. 170. Wiley. New York, N.Y.

13. MacDonald, A.D. Microwave Breakdown in Gases. 122. Wiley. New York, N.Y.

14. Allis, W.P. 1956. Motions of Ions and Electrons. In Handbuch der Physik. S. Flügge, Ed. Vol. 21. 383 - 444. Springer-Verlag. Berlin.

Figure Captions

Fig. 1. (a) Plot of Φ in one quadrant of an axial midplane cross section of the cylindrical cavity. (b) Plot of the field in the axial midplane of the cylindrical cavity. The dashed line outline of the Φ potential well corresponds to the dotted line isopotential in Fig. 1(a).

Fig. 2. Plot of a computer-simulated trajectory of a single electron confined in the axial midplane of the TM_{011} mode. The electron was launched at the point indicated by the arrow. The trajectory was computed for 500 cycles of the cavity field.

Fig. 3. Cross section diagram of the resonant cavity used.

Fig. 4. Photograph of the resonant cavity.

Fig. 5. Block diagram of the experimental system.

Fig. 6. Photograph of the experimental system. From left to right, the major units are the klystron power amplifier, a rack of frequency-measuring equipment, the automatic impedance plotter, the klystron control console, the resonant cavity sitting on top of the sound-suppressing enclosure surrounding the turbomolecular pump, and a rack of vacuum gauge circuits.

Fig. 7. Breakdown curves for TM_{010} and TM_{011} modes.

Fig. 8. Photographs of plasmas in a semi-transparent resonant cavity and diagrams of the fields used to excite the plasmas.

Fig. 9. Diagram of pivoted photometer arrangement used to record axial luminosity distribution of plasma.

Fig. 10. Luminosity profiles for TM_{011} mode. Trace A corresponds to A in Fig. 7 in the non-confining diffusion regime. Trace B corresponds to B in Fig. 7 in the confining regime.

Fig. 11. Diagram showing probe used to measure plasma floating potential at central nodal point in cavity.

Fig. 12. Plot of plasma floating potential and cavity rf field vs. pressure.

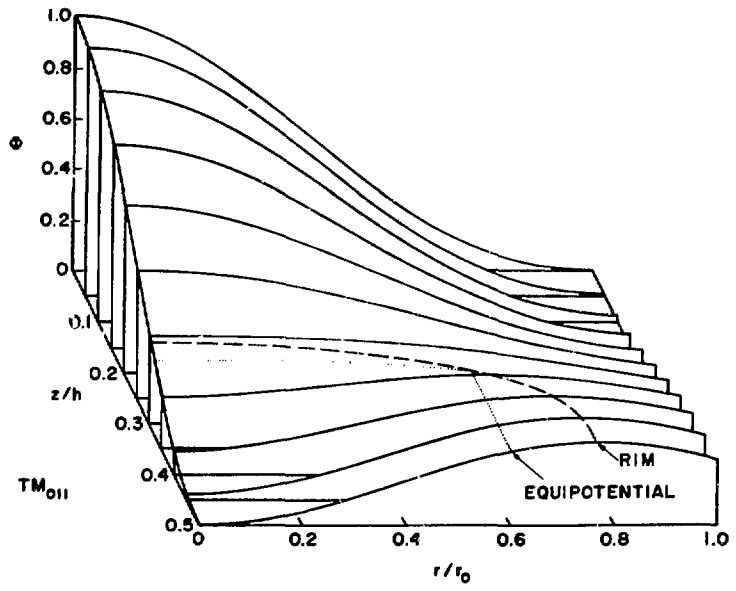
1.0
0.8
0.6
0.4
0.2
0
Φ
0.1
0.2
z/h
0.3
0.4
0.5
TM011
0
0.2
0.4
0.6
0.8
1.0
r/r0
RIM
EQUIPOTENTIAL

Fig. 1 (a)

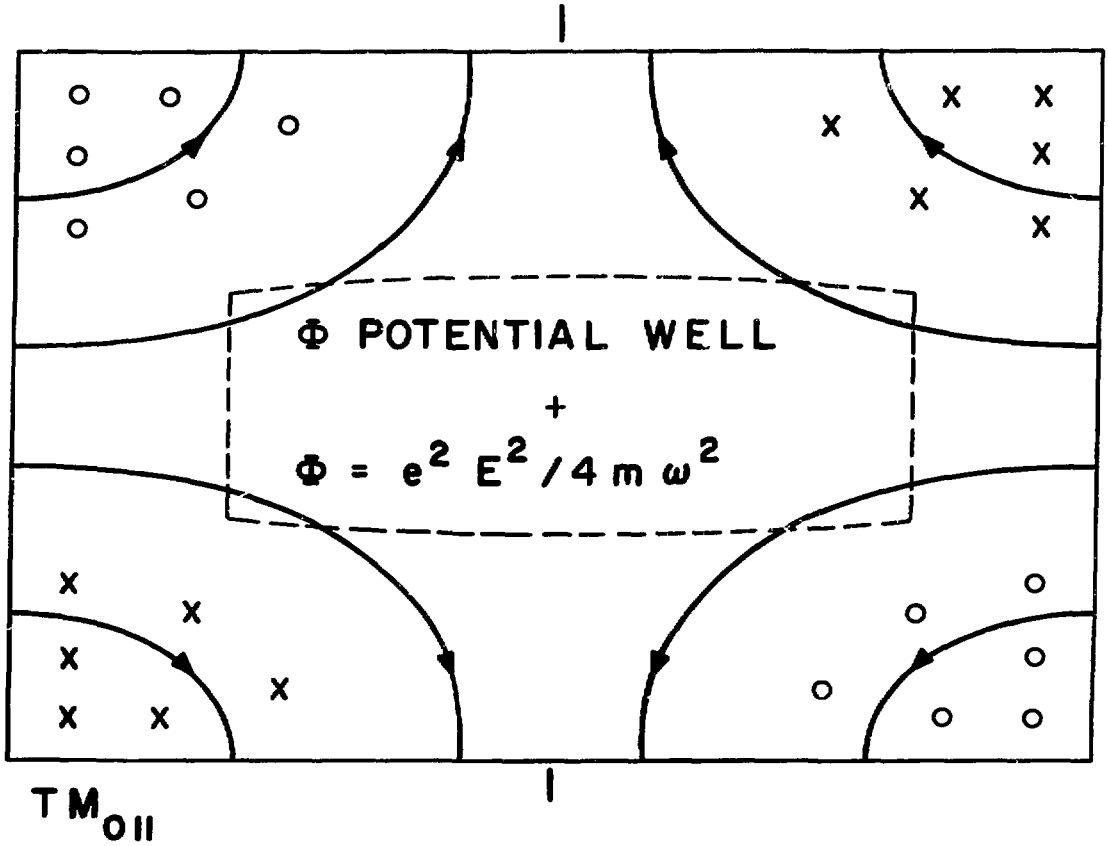

Fig. 1 (b)

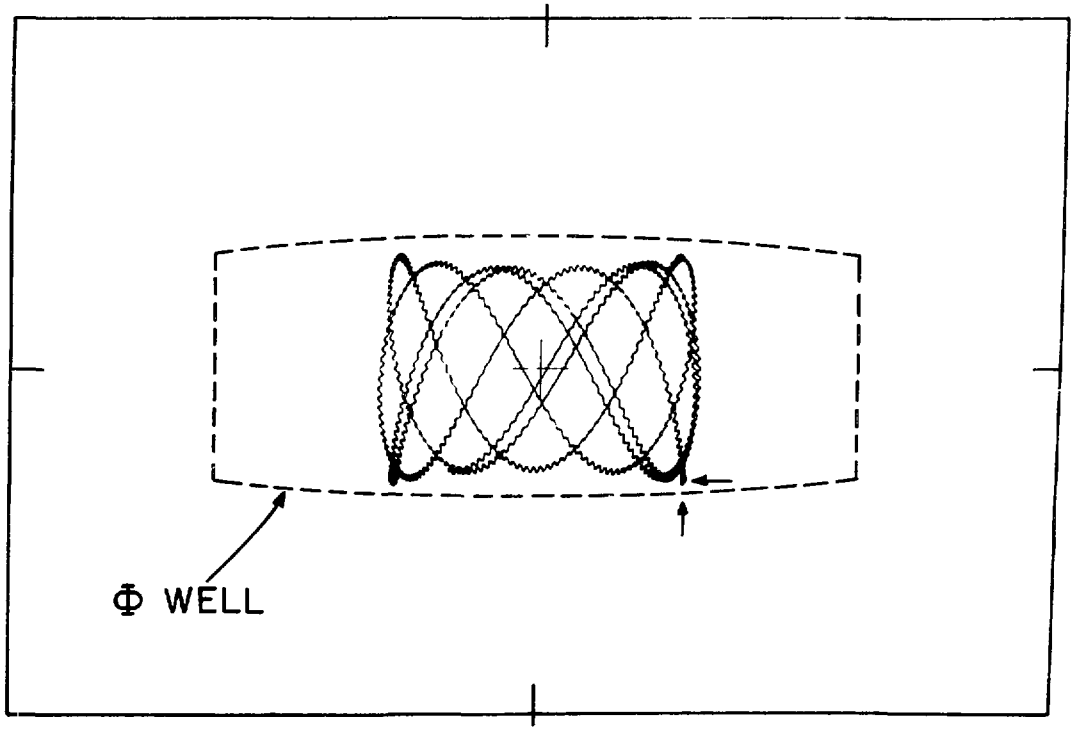

Fig. 2

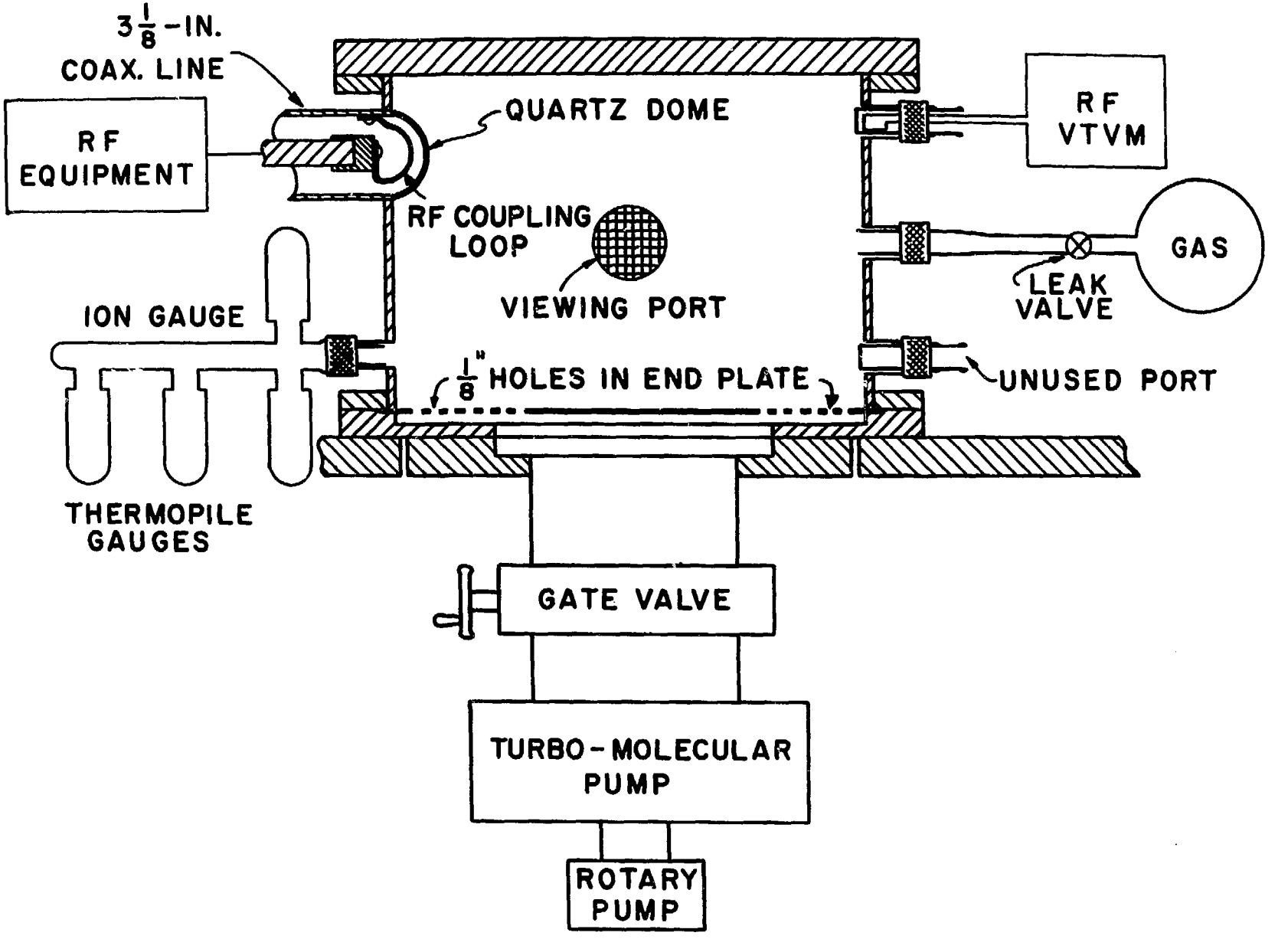
3 1/8 - IN.
COAX. LINE
RF
EQUIPMENT
QUARTZ DOME
RF
VTVM
RF COUPLING
LOOP
GAS
VIEWING PORT
LEAK
VALVE
ION GAUGE
1/8" HOLES IN END PLATE
UNUSED PORT
THERMOPILE
GAUGES
GATE VALVE
TURBO - MOLECULAR
PUMP
ROTARY
PUMP

Fig. 3

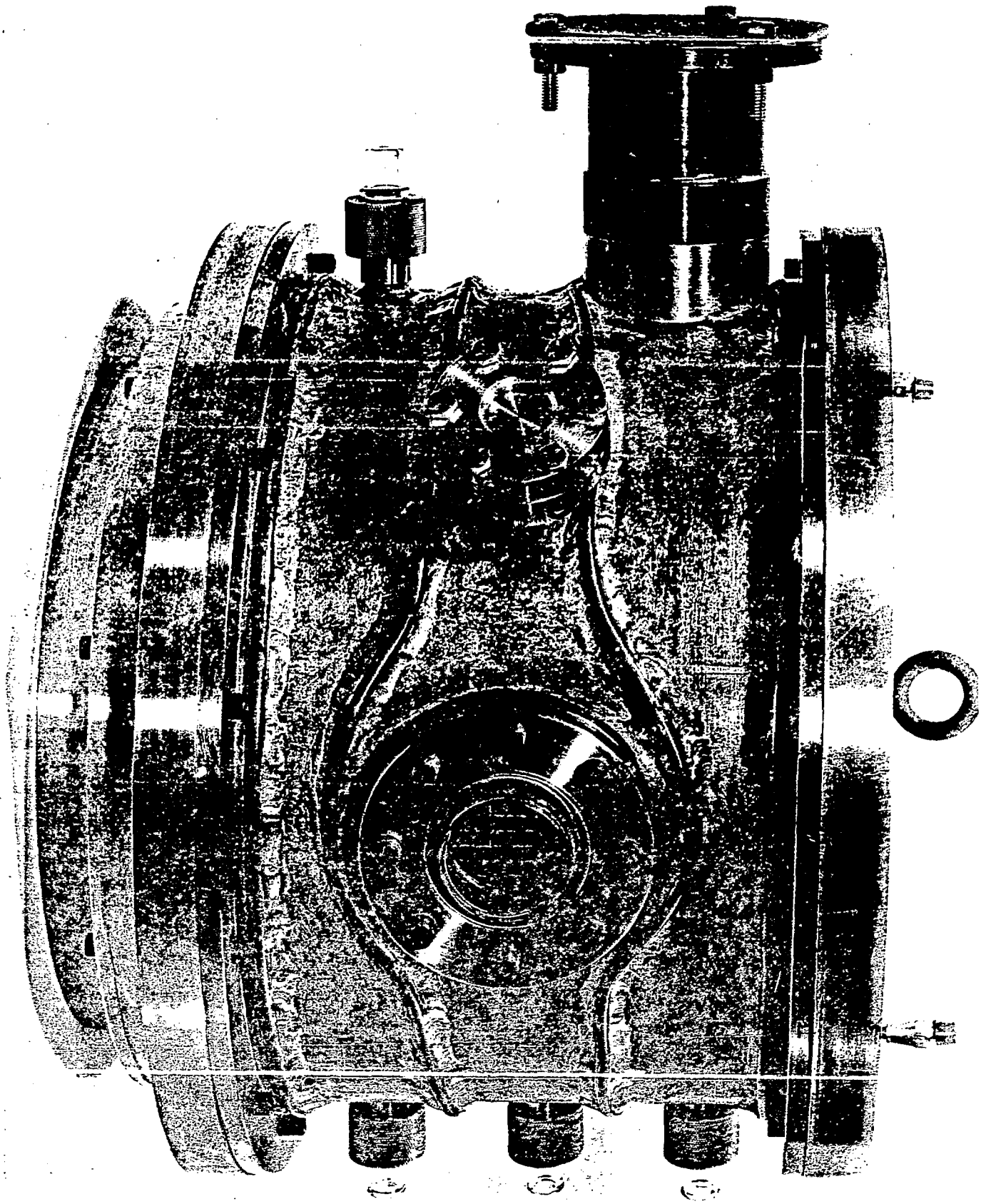

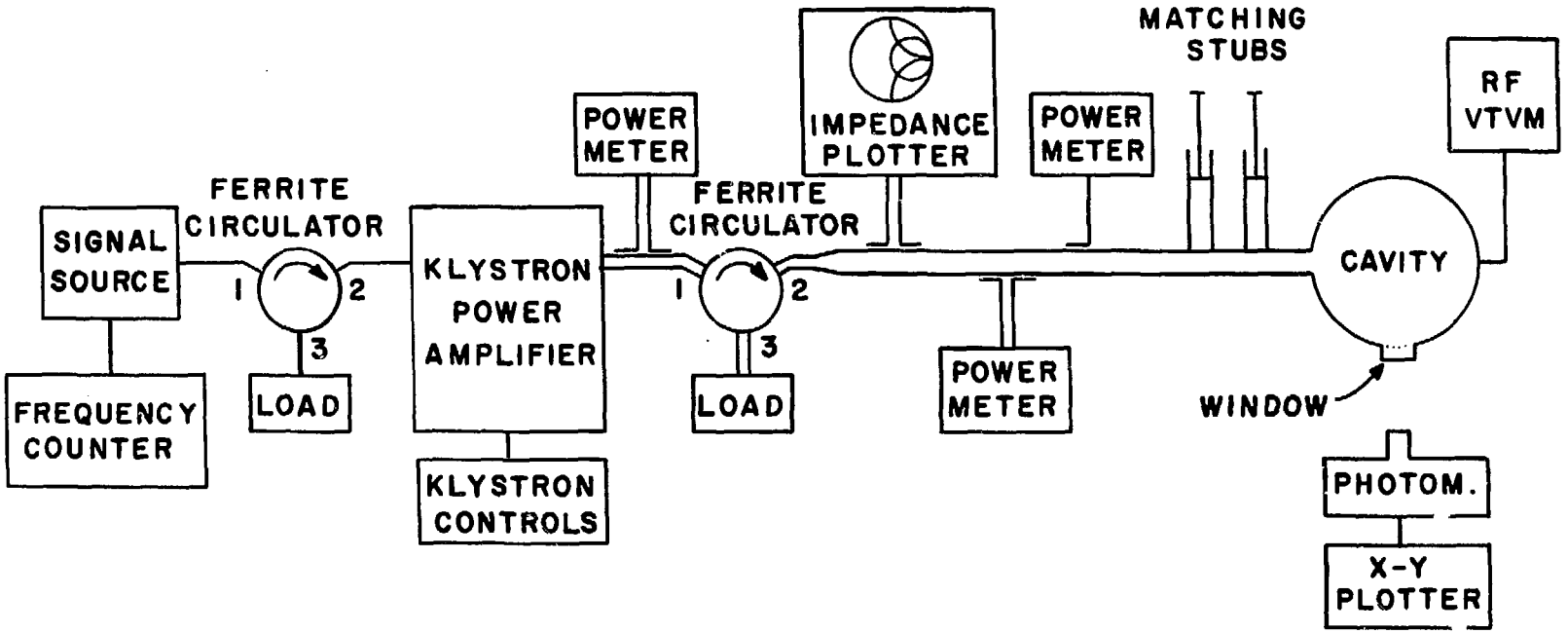
SIGNAL SOURCE
FREQUENCY COUNTER
FERRITE CIRCULATOR
1
2
3
LOAD
KLYSTRON POWER AMPLIFIER
KLYSTRON CONTROLS
POWER METER
IMPEDANCE PLOTTER
FERRITE CIRCULATOR
1
2
3
LOAD
POWER METER
POWER METER
MATCHING STUBS
RF VTVM
CAVITY
WINDOW
PHOTOM.
X-Y PLOTTER

Fig. 5

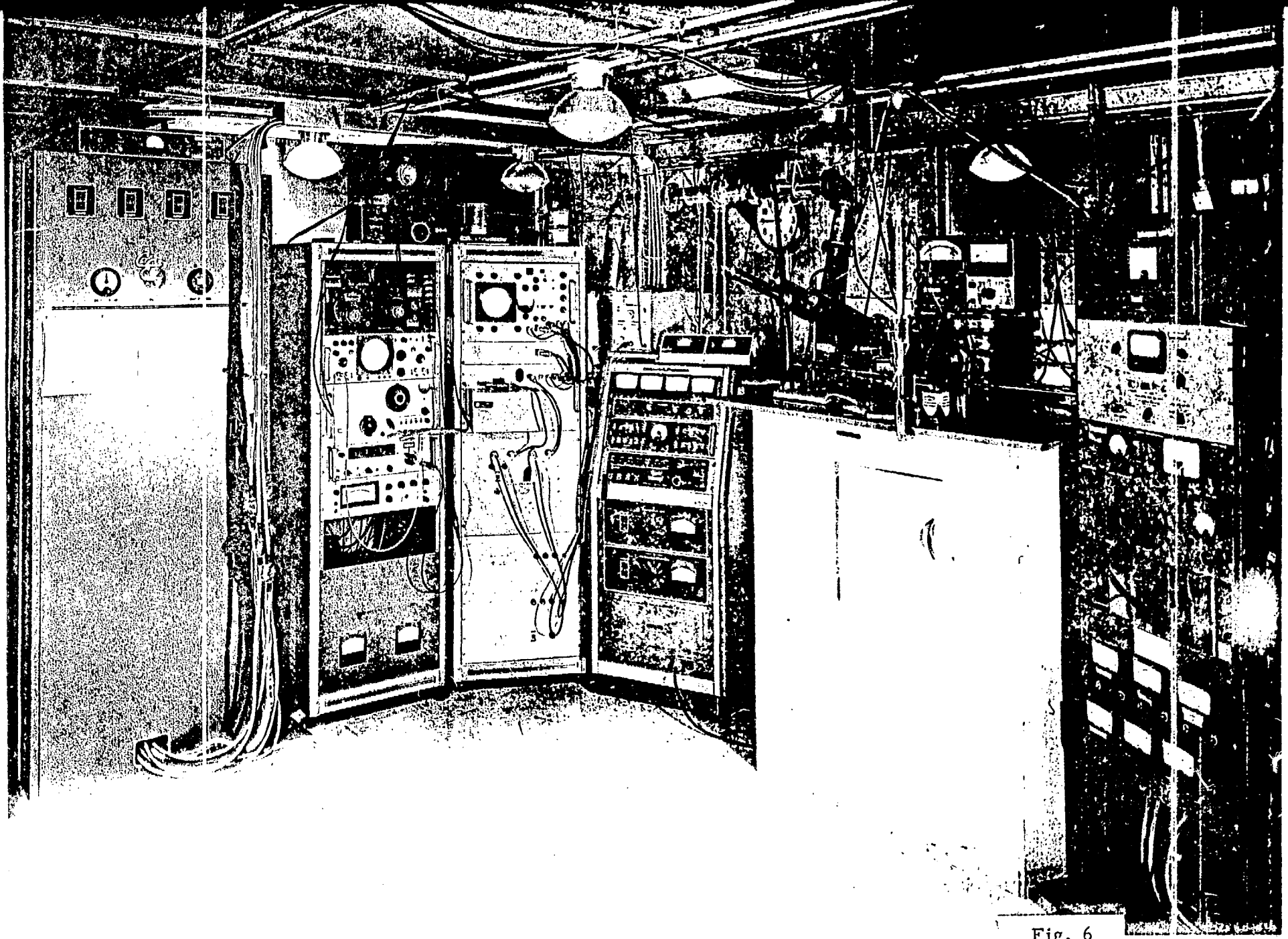

Fig. 6

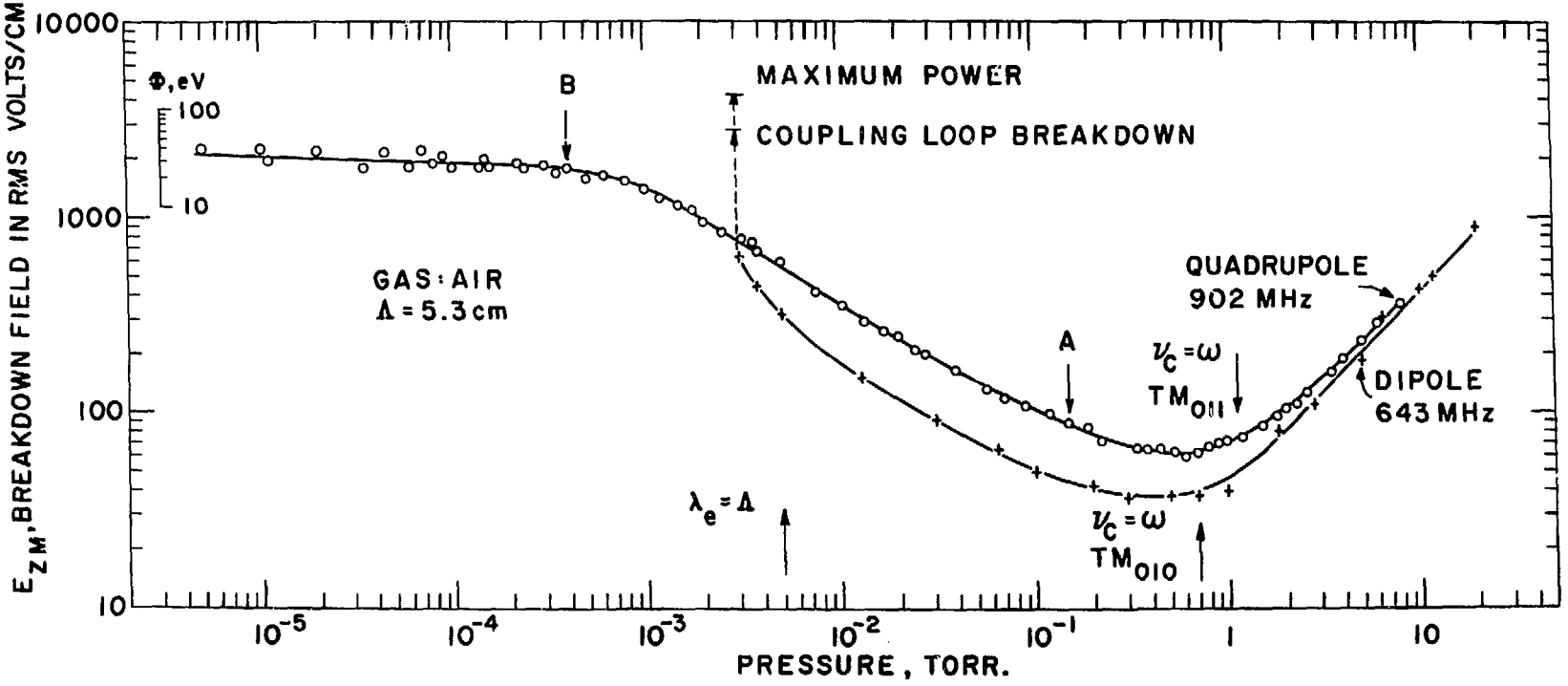
E_{ZM}, BREAKDOWN FIELD IN RMS VOLTS/CM
10000
1000
100
10
Φ, eV
100
10
B
MAXIMUM POWER
COUPLING LOOP BREAKDOWN
GAS: AIR
Λ = 5.3 cm
QUADRUPOLE
902 MHz
A
$\nu_c = \omega$
TM_{011}
DIPOLE
643 MHz
$\lambda_e = \Lambda$
$\nu_c = \omega$
TM_{010}
10^{-5}
10^{-4}
10^{-3}
10^{-2}
10^{-1}
1
10
PRESSURE, TORR.

Fig. 7

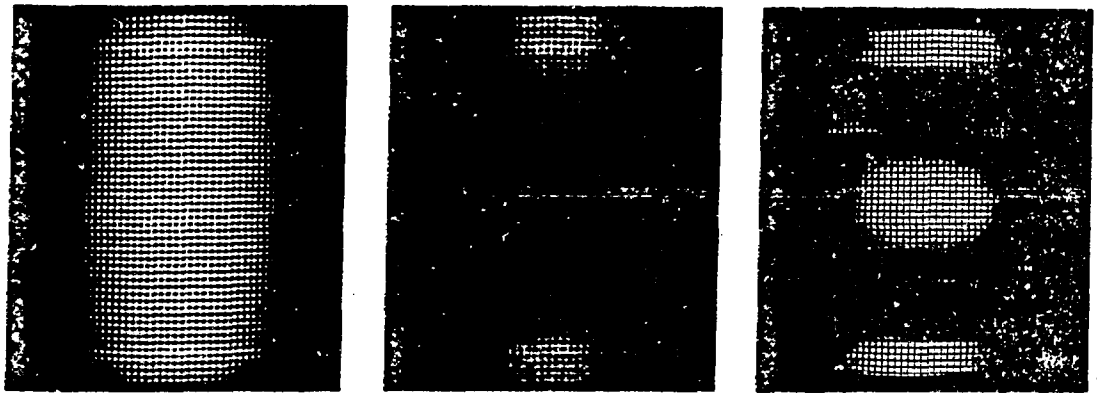

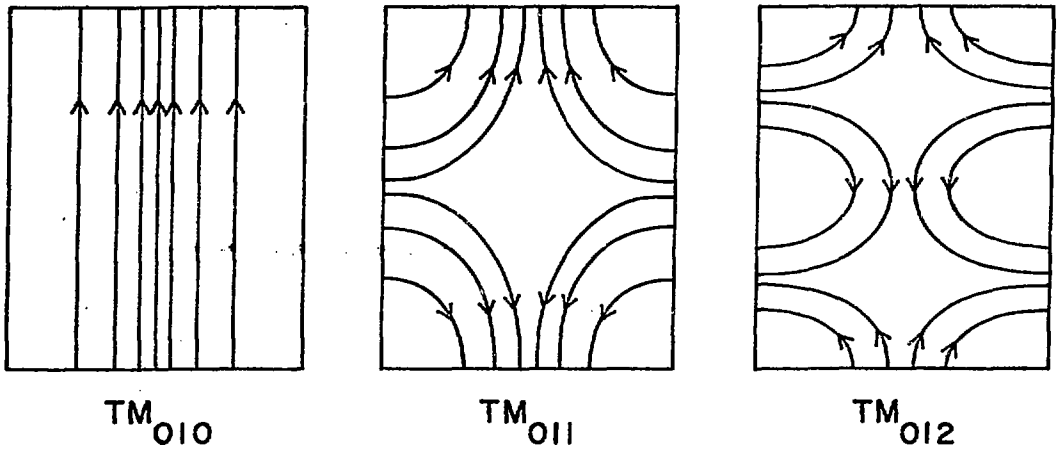

Fig. 8

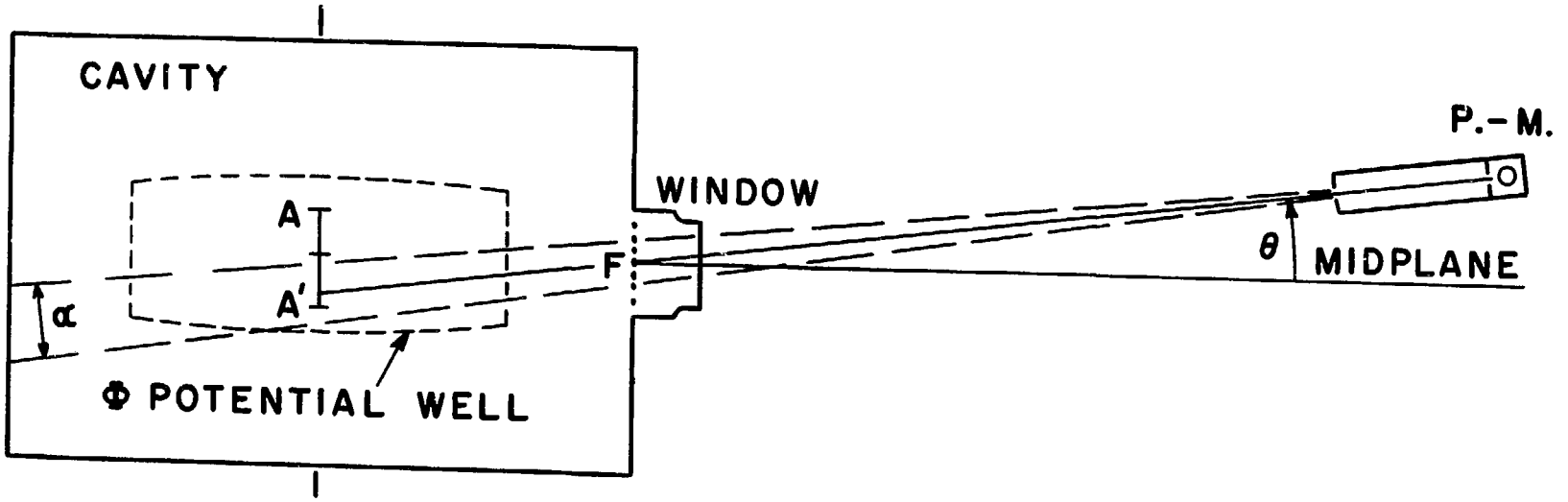

Fig. 9

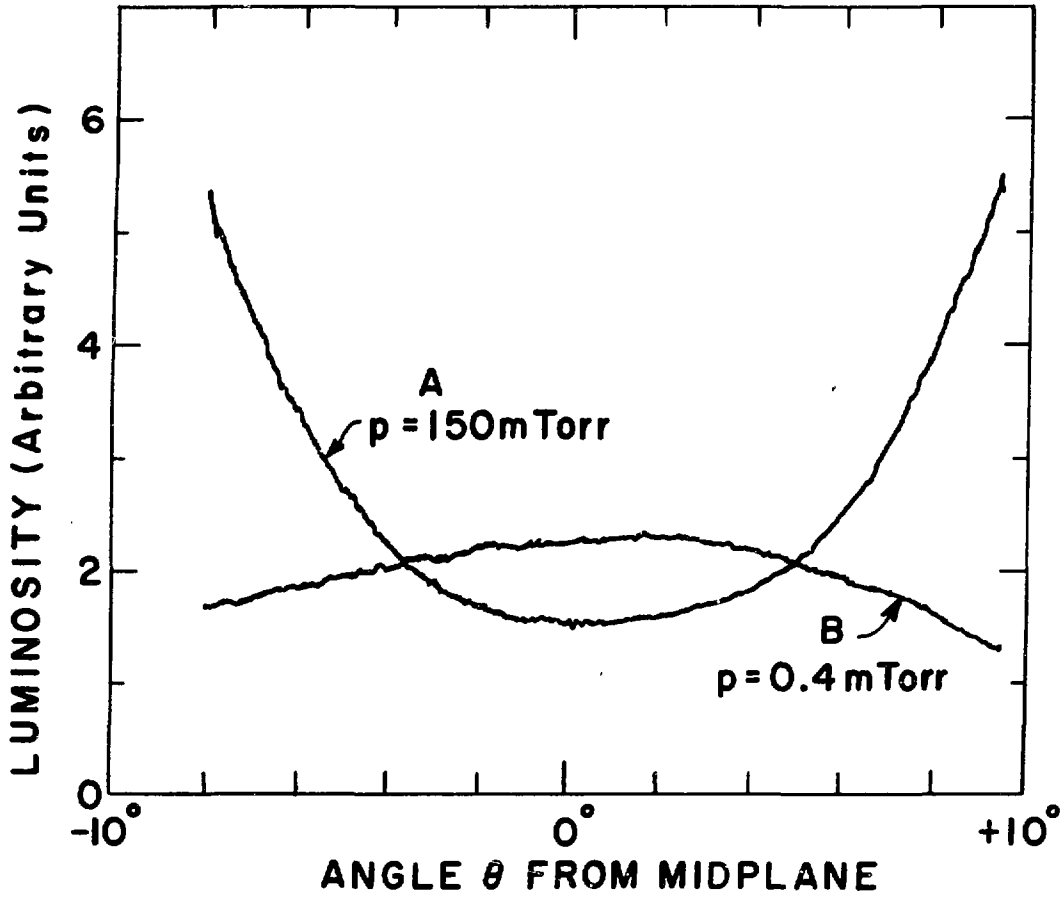
LUMINOSITY (Arbitrary Units)
6
4
2
0
A
p = 150mTorr
B
p = 0.4 mTorr
-10°
0°
+10°
ANGLE θ FROM MIDPLANE

Fig. 10

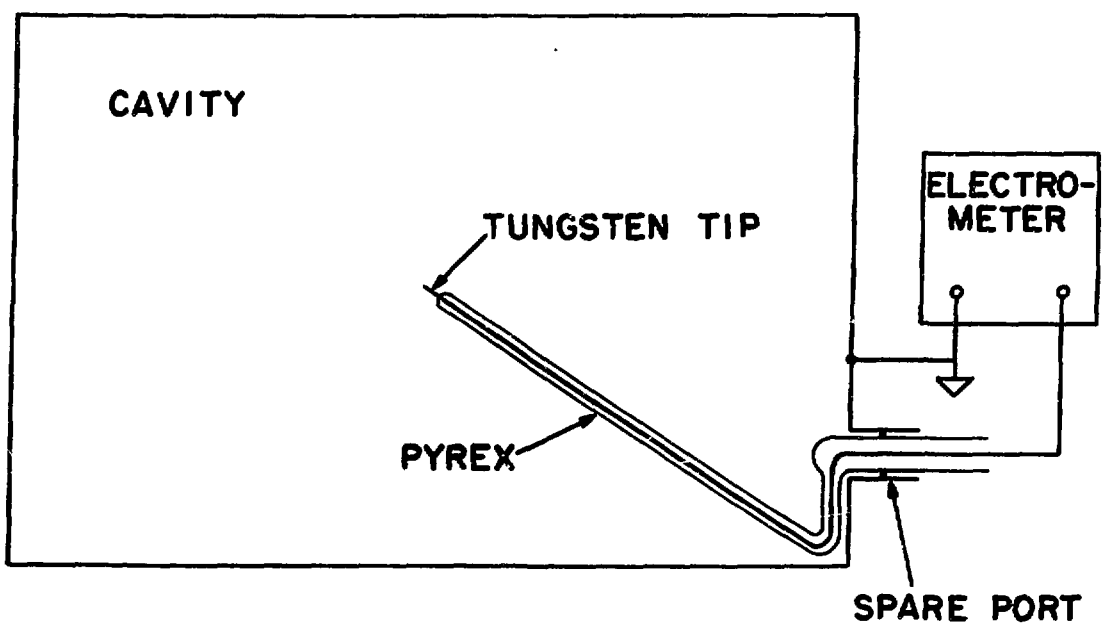

Fig. 11

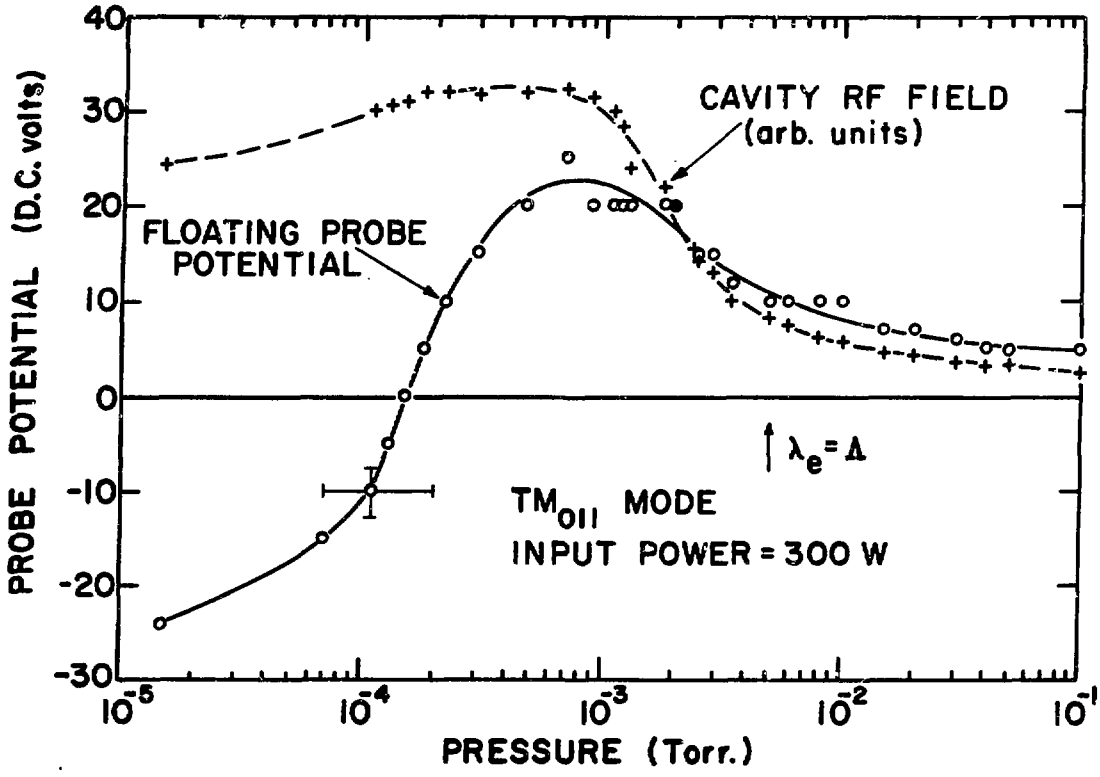
40
30
20
10
0
-10
-20
-30
PROBE POTENTIAL (D.C. volts)
CAVITY RF FIELD
(arb. units)
FLOATING PROBE
POTENTIAL
$\lambda_e = \Lambda$
TM_{011} MODE
INPUT POWER = 300 W
10^{-5}
10^{-4}
10^{-3}
10^{-2}
10^{-1}
PRESSURE (Torr.)

Fig. 12